Granular Matter (2008) 10:63–73
DOI 10.1007/s10035-007-0077-8

Granular temperature in a gas fluidized bed

Mark J. Biggs · Don Glass · L. Xie · Vladimir Zivkovic · Alex Buts · M. A. Curt Kounders

Received: 25 February 2007 / Published online: 6 November 2007

Abstract The mean square of particle velocity fluctuations, δv^2, which is directly related to the so-called granular temperature, plays an important role in the flow, mixing, segregation and attrition phenomena of particulate systems and associated theories. It is, therefore, important to be able to measure this quantity. We report here in detail our use of diffusing wave spectroscopy (DWS) to measure the mean square particle velocity fluctuations for a 2D non-circulating gas fluidized bed of hollow glass particles whose mean diameter and effective density are 60 μm and 200 kg/m^3, respectively. Mean square particle velocity fluctuations were observed to increase with superficial velocity, U_s, beyond the minimum fluidization velocity. Following the uniform fluidization theory of Batchelor (1988), the function $f(\phi)$ in the expression $\delta v^2 = f(\phi)U_s^2$ was also determined and shown to increase from zero at a solids loading of $\phi \approx 0.33$ to a maximum at $\phi \approx 0.4$ before decreasing again to zero at $\phi \approx 0.53$. The spatial variation of the mean square particle velocity fluctuations was also determined and shown to be approximately symmetrical about the centreline where it is also maximal, and to increase with height above the distributor.

Keywords Granular temperature · Velocity fluctuations · Kinetic theory · Erosion · Heat transfer · Granulation · Diffusing wave spectroscopy · Fluidized bed

M. J. Biggs (✉) · D. Glass · L. Xie · V. Zivkovic · A. Buts
Institute for Materials and Processes, University of Edinburgh, King's Buildings, Mayfield Road, Edinburgh EH9 3JL, Scotland, UK
e-mail: M.Biggs@ed.ac.uk

M. A. Curt Kounders
School of Mathematics, Kingston University, Penrhyn Road, Kingston-on-Thames, KT1 2EE Surrey, England, UK

1 Introduction

Granular flows in which the particulate motion involves successive ballistic flights between predominately binary collisions occur widely—just two examples are fluidization and pneumatic conveying of powders. The similarity between such "rapid granular flow" and the behaviour of dense gases has lead to the development of inelastic kinetic theories [1–4] akin to those established for the former many years ago [5,6]. There are a number of key fundamental quantities required for the evaluation of the constitutive parameters of these theories. One of them is the so-called "granular temperature", which is a quantity that is proportional to the square of the particle velocity fluctuations about the mean [1,2]. The central role played by this quantity in the kinetic theories of rapid granular flow [7] and models for other phenomena (e.g. heat transfer [8], granulation [9] and erosion [10]) in such flows means the validation of these theories requires its measurement.

A range of methods have been used over the past 15 or more years to measure the granular temperature for a variety of systems. The first attempts involved use of fibre optic probes to measure streamwise velocity fluctuations in 3D chute flows [11,12], a method also used later to study granular flow in a rotating drum [13]. The intrusive nature of this method and its restriction to a single direction means it has seen limited application. Computer-aided analysis of video images is the most widely used non-intrusive means of determining granular temperature—it has been used to study granular flows down chutes [14–19], granular materials undergoing slow shear [20–26] and a variety of fluidized beds [27–37]. The restriction of the video image analysis approach and other optical methods such as laser Doppler velocimetry [38] to dilute systems or the surfaces of dense systems has motivated some to develop the application of

radioactive particle tracking methods [39–43] and nuclear magnetic resonance (NMR) [44,45]. These methods are not well suited for the study of dense systems involving small particles and/or high particle speeds, however. In these situations, indirect non-intrusive methods can be used such as the shot-noise method of Cody et al. [46], diffusing-wave spectroscopy (DWS) [47–51] and inversion of solid pressure fluctuation data [52–54], or indirect intrusive methods such as that of Mayor and co-workers [55–57].

Only a small number of studies have focused on non-circulating fluidized beds (nc-FBs), which are of particular interest here. The most comprehensive study to date is that of Cody et al. [46], who measured the granular temperature of a range of different particles in FBs made of different materials. Amongst other things, these workers found that the variation of velocity fluctuations, δv, with superficial velocity, U_s, for different "classes" of particles can be reduced to a reasonable degree by the dimensionless group $\left(\delta v / U_s\right)\left(d_p / d_0\right)$, where d_p is particle diameter and $d_0 = 110\,\mu\text{m}$ is an empirical characteristic length scale that is possibly a function of the particle material amongst other factors. Granular temperature data for a variety of Geldart Group A (and smaller Geldart Group B) particles reduced using this group was found to increase sharply to a maximum once the superficial velocity exceeded the minimum fluidization velocity, U_{mf}, before decaying in an exponential manner to $\sim$1 at $U_s / U_{mf} \approx 10$.

A second notable study of granular temperature in nc-FBs is that of Menon and Durian [48], who used DWS to determine the granular temperature of Geldart Group A and Group B particles. Whilst these workers claimed their results to be qualitatively similar to those of Cody et al. [46], they differed in one critical respect at the very least—they only observed particle velocity fluctuations when bubbling was present. The sensitivity of DWS—it can in principle detect motion at extremely short length (1–10 nm) and time (10 ns) scales—led Menon and Durian to claim that nc-FBs are a static network of particles (i.e. a solid) in the absence of bubbling. This contention is not supported, however, by other more recent work—Spinewine et al. [33] observed particle velocity fluctuations directly in a water fluidized bed of 6.1 mm particles, whilst Valverde et al. [58] observed particle diffusion in a gas nc-FB of 8.53 μm flow-conditioned toner particles.

Unlike many of the other granular systems considered to date, there is no understanding of how the granular temperature varies spatially within nc-FBs. Additionally, no attempt has been made to deconvolute the effect of superficial velocity and bed voidage on granular temperature. In an effort to address both these issues as well as clarify the work of Menon and Durian [48], we have applied DWS to a nc-FB of particles for which $U_{mb} \gg U_{mf}$. We first outline the experimental approach adopted, including a brief description of diffusing wave spectroscopy, details of the experimental apparatus and methodology used, and the nature of the fluidized material. This is followed by a brief consideration of the mean square displacement of the particles in the bed and the autocorrelation functions from which it is determined. The variation of granular temperature with superficial velocity and voidage are then considered. Finally, the spatial variation of granular temperature is presented and explained.

2 Experimental details

2.1 Granular temperature from diffusing wave spectroscopy

Diffusing wave spectroscopy [59] provides a means of determining the mean square displacement (MSD), $\langle \Delta r^2(t) \rangle$, of the particles in a *non-dilute* dispersed phase medium such as a colloid or bulk solid. The mean particle fluctuating velocity, δv^2, can be derived from the short-time region of the MSD where ballistic motion occurs; i.e.

$$\lim_{t \to 0} \langle \Delta r^2(t) \rangle = \langle \delta v^2 \rangle t^2 \tag{1}$$

The first step in the process of determining the MSD of the particles is to measure the time variation of the intensity of light that has passed through the medium. This intensity variation, $I(t)$, is then used to evaluate the autocorrelation function of the light intensity

$$g_2(t) = \frac{\langle I(0) I(t) \rangle}{\langle I(0) \rangle^2} \tag{2}$$

The normalised electric field autocorrelation function, $g_1(t)$, is then obtained using the Siegert relationship [59]

$$g_2(t) = 1 + \beta |g_1(t)|^2 \tag{3}$$

where β is a free parameter determined during the fitting.

The normalised electric field autocorrelation function can be related to the MSD by first relating the latter to the change in phase of the light, and then modelling the light propagation through the medium by a diffusion process, which is a good assumption provided the photons experience many scattering events as they transverse the medium. The exact nature of this relationship between $g_2(t)$ and $\left\langle \Delta r^2(t) \right\rangle$ depends on various factors such as the configurations of the light source and detector, the geometry of the medium, and its optical properties. Of particular interest here is the case illustrated in Fig. 1, where a plane light source of wavelength, λ, falls on one side of a light-absorbing medium whose thickness, L, is much less than the other dimensions and where the scattered light is collected from a point either on the same side as the incident light source (backscattering) or the opposite side (transmission). In the latter case, the relationship is [59]

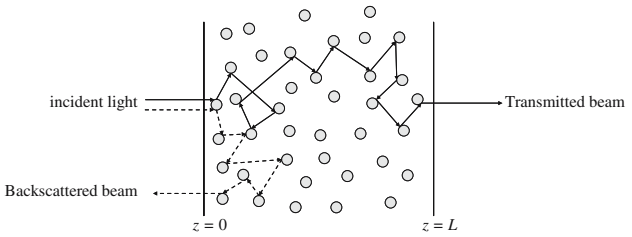

Fig. 1 Schematic of the process that underpins diffusing wave spectroscopy. A beam of light incident on the dispersed phase medium is multiply scattered by the moving particles (shown as *grey circles*) before exiting the medium to be picked up by light intensity detectors. The light that exits from the face on which the incident beam enters is said to be backscattered, whilst that which leaves through the opposite face is said to be transmitted—both beams can be analysed to determine the granular temperature provided the signal-to-noise ratio is adequate

data and, therefore, the values for the transport mean free path and absorption path length [50].

2.2 Experimental set-up

The experimental apparatus, which is illustrated in Fig. 2, was located in a temperature and humidity controlled laboratory. Two-dimensional fluidized beds were used to facilitate DWS in both the transmission and backscattering modes. The beds were each constructed from two scratch-resistant glass plates mounted in an aluminium frame. The fluidized bed for which the granular temperature data was determined—which is henceforth termed the "primary" FB—was 8.422 mm thick, 600 mm high and 194 mm wide. Four other FBs of similar construction but different thicknesses (5.438, 7.726, 10.322 and 12.066 mm) were additionally used in determining the transport mean free path and absorption path length. Compressed air from a pressure regulated compressor was introduced to the beds through a wind box below a sintered metal

$$g_1(t) = \frac{\frac{L/l^*+4/3}{z_0/l^*+2/3}\left[\sinh\left(\frac{z_0}{l*}\sqrt{k_0^2\langle\Delta r^2\rangle+\frac{3l^*}{l_a}}\right)+\frac{2}{3}\sqrt{k_0^2\langle\Delta r^2\rangle+\frac{3l^*}{l_a}}\cosh\left(\frac{z_0}{l*}\sqrt{k_0^2\langle\Delta r^2\rangle+\frac{3l^*}{l_a}}\right)\right]}{\left(1+\frac{4}{9}k_0^2\langle\Delta r^2\rangle+\frac{4l^*}{3l_a}\right)\sinh\left(\frac{L}{l^*}\sqrt{k_0^2\langle\Delta r^2\rangle+\frac{3l^*}{l_a}}\right)+\frac{4}{3}\sqrt{k_0^2\langle\Delta r^2\rangle+\frac{3l^*}{l_a}}\cosh\left(\frac{L}{l^*}\sqrt{k_0^2\langle\Delta r^2\rangle+\frac{3l^*}{l_a}}\right)} \tag{4}$$

where l^* is the transport mean free path, l_a is the absorption path length, z_0 is the distance over which the *incident* light is randomized, and $k_0 = 2\pi/\lambda$. In the backscattering mode, the appropriate expression, which is only valid at short times in this case, is [59]

$$g_1(t) = \frac{\sinh\left(\sqrt{k_0^2\Delta r^2+\frac{3l^*}{l_a}}\left(\frac{L}{l^*}-\frac{z_0}{l^*}\right)\right)+\frac{2}{3}\sqrt{k_0^2\langle\Delta r^2\rangle+\frac{3l^*}{l_a}}\cosh\left(\sqrt{k_0^2\langle\Delta r^2\rangle+\frac{3l^*}{l_a}}\left(\frac{L}{l^*}-\frac{z_0}{l^*}\right)\right)}{\left(1+\frac{4}{9}k_0^2\langle\Delta r^2\rangle+\frac{4l^*}{3l_a}\right)\sinh\left(\frac{L}{l^*}\sqrt{k_0^2\langle\Delta r^2\rangle+\frac{3l^*}{l_a}}\right)+\frac{4}{3}\sqrt{k_0^2\langle\Delta r^2\rangle+\frac{3l^*}{l_a}}\cosh\left(\frac{L}{l^*}\sqrt{k_0^2\langle\Delta r^2\rangle+\frac{3l^*}{l_a}}\right)} \tag{5}$$

Given the normalised electric field autocorrelation function, Eqs. (4) or (5) can be inverted to obtain the MSD of the particles provided l^*, l_a and z_0 are known for the medium. The transport mean free path, l^*, which is the distance that a photon must travel *within* the medium before its direction is completely randomised, and the absorption path length, l_a, which is a measure of the distance photons will travel before being absorbed, are determined from independent measurement of the variation of the transmitted light intensity with the thickness of the medium, $I(L)$, using the equation [60,61]

$$\frac{I(L)}{I_0} = \frac{\sinh\left[\frac{z_0}{l_a}+\frac{1}{2}\ln\left(\frac{l_a+\beta l^*}{l_a-\beta l^*}\right)\right]\sinh\left[\frac{1}{2}\ln\left(\frac{l_a+\beta l^*}{l_a-\beta l^*}\right)\right]}{\frac{1}{2}\ln\left(\frac{l_a+\beta l^*}{l_a-\beta l^*}\right)\sinh\left[\frac{L}{l_a}+\ln\left(\frac{l_a+\beta l^*}{l_a-\beta l^*}\right)\right]} \tag{6}$$

where β is a constant that accounts for reflections at the interfaces of the vessel containing the medium. The distance over which the incident light is randomized, z_0, is normally assumed to scale directly with the transport mean free path; i.e. $z_0 = \gamma l^*$. Whilst reliable estimates for the scaling constant are difficult to obtain, use of $\gamma = 1$ and $\gamma = 5/3$, which are two common values cited in the literature [59,62], lead to no perceptible change in the fit of Eq. (6) to our experimental

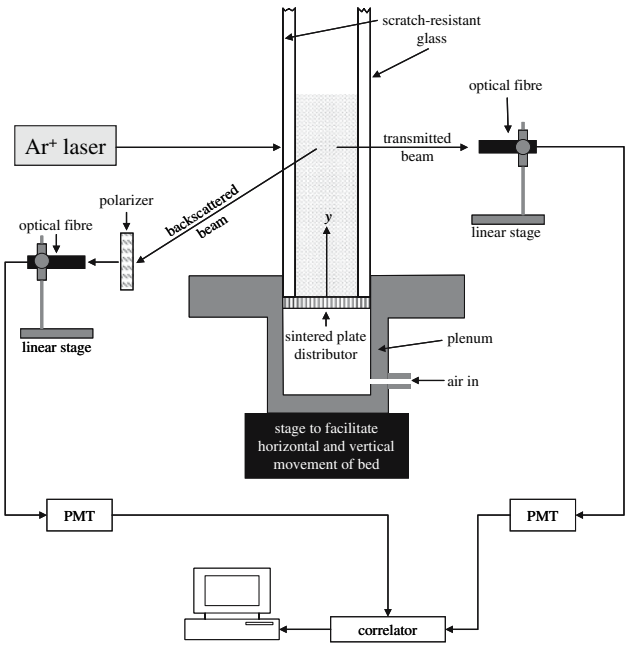

Fig. 2 Schematic showing the experimental apparatus for determining the granular temperature distribution in a gas fluidized bed

gas distributor. The air flow rate to the beds was metered by needle valves and rotameters. The beds were fixed on a stage whose vertical and horizontal position could be adjusted to permit study along the height, y, and across the width, x, of the beds whilst leaving the optical arrangements undisturbed.

The beds were illuminated by a Coherent Innova 90 argon laser of wavelength $\lambda = 514.5$ nm and beam diameter $\sim$2.5 mm. Both the backscattered and transmitted light were collected by optical fibres connected to separate photomultiplier tubes (PMTs). The fibres were mounted in linear stages so that their height could be adjusted accurately and with ease. The output from the PMTs were connected to separate channels of an ALV-5000E digital correlator (ALV GmbH, Germany) which evaluated the intensity autocorrelation functions of both signals in real time before being stored on a PC for later processing. So as to avoid sampling of photons that had only been subject to a small number of scattering events, the backscattered light was filtered using a polarizer perpendicular to the incident laser beam polarization.

2.3 Fluidized material

One possible reason why Menon and Durian [48] did not *observe* velocity fluctuations prior to onset of bubbling was the very small interval between the minimum fluidisation and minimum bubbling velocities for the particles they considered [58]. Valverde and co-workers [58] addressed this issue by using 8.53 μm diameter particles. Use of this size of particle required addition of flow conditioners, however [58]. So as to avoid the need to use flow conditioners here, we have used much larger hollow glass particles of significantly lower density (Q-Cel® 5020, PQ Corporation). The bulk and effective densities of the particles were $\rho_b = 110$ kg/m^3 and $\rho_e = 200$ kg/m^3 respectively, whilst analysis using a Malvern Mastersizer S particle size analyzer indicated the particle sizes were distributed between 20 and 100 μm with an average of $d_p = 60$ μm.

A typical variation of the relative bed expansion, $(h - h_0)/h_0$, and pressure drop across the bed, ΔP, with superficial velocity is shown in Fig. 3. The pressure drop across the bed increases sharply from zero with superficial velocity until bed expansion is first seen where its rate of increase diminishes to a plateau at $U_s \approx 4.5$ mm/s. The pressure drop across the bed beyond this point is approximately 5% less than the weight of the bed, indicating weak cohesive forces are at play.

Figure 4 shows that the nature of the fluidization changed with superficial velocity, with isolated channelling occurring just above $U_s \approx 1.4$ mm/s followed by increased channelling with isolated localised bulk motion, then non-uniform fluidization and, finally, uniform fluidization beyond $U_s \approx 4.8$ mm/s. The various transitions which followed channelling occurred first at the top of the bed before propagating downwards to the distributor. Bubbling was first visually observed

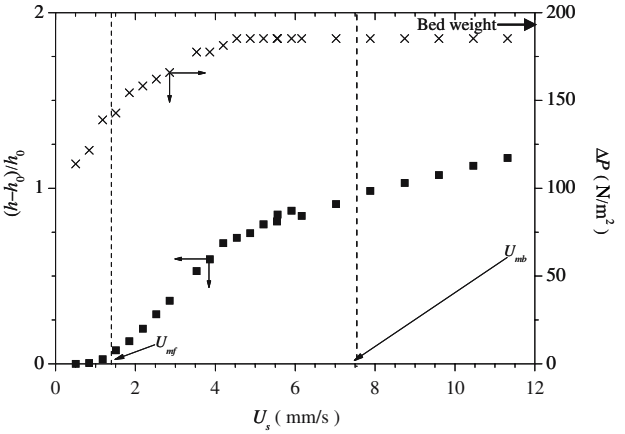

Fig. 3 Typical bed expansion (*squares*) and pressure drop (*crosses*) variation with superficial velocity. Absence of *error bars* indicates the errors are no greater than the size of the symbol. The observed minimum fluidization velocity, $U_{mf} = 1.4 - 1.5$ mm/s, and minimum bubbling velocity, $U_{mb} = 7.5$ mm/s are both shown

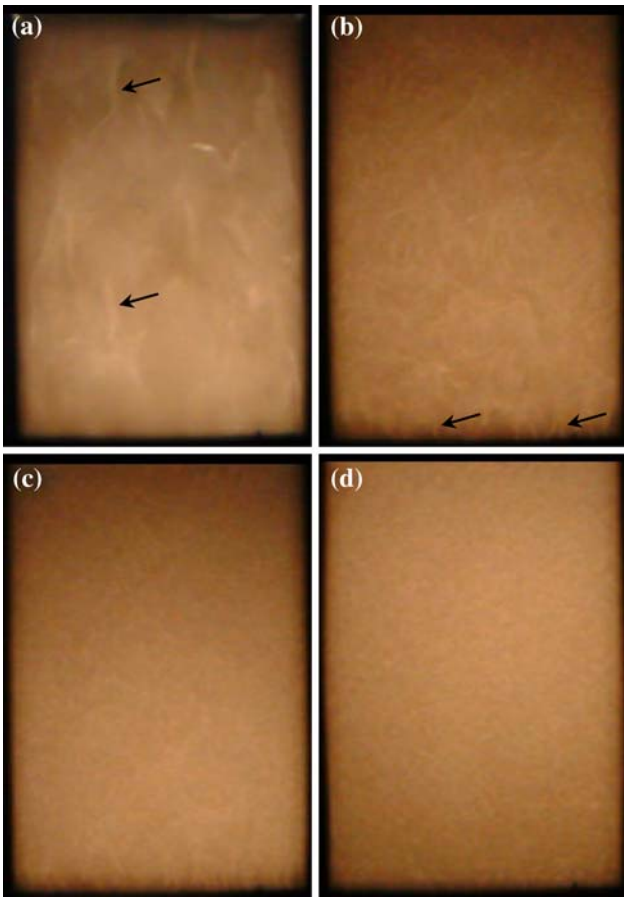

Fig. 4 Images of fluidized particles at: **a** $U_s/U_{mf} = 1.33$; **b** $U_s/U_{mf} = 2.50$; **c** $U_s/U_{mf} = 4.33$; and **d** $U_s/U_{mf} = 8.33$. The *arrows* indicate examples of the channels observed in the bulk of the bed at low superficial velocities and at the base of the bed at moderate superficial velocities. The channels may be more clearly seen in the colour version of the paper found online

at a relative bed expansion of ∼100% and superficial velocity of ∼7.5 mm/s. This observed bubbling velocity corresponds very well to the upper limit of the experimental data that is well modelled (correlation coefficient of 0.997) by the Richardson–Zaki correlation, $U_s U_t = \varepsilon^n$, where U_t is the terminal velocity of the average particle size, and ε is the bed voidage. The value of the exponent obtained from the fit, $n = 6.94$, is greater than that associated with liquid FBs in the limit of low particle Reynolds number (4.65) for which the Richardson–Zaki correlation is normally applied, but it does agree with those obtained by others for gas-fluidized Geldart class A and C particles [63].

Defining the minimum fluidization velocity, U_{mf}, is not straightforward for the system considered here. If onset of fluidization is considered to occur where bed height first changes, then U_{mf} would be 1.4–1.5 mm/s. If, however, it is considered to occur where the pressure drop across the bed ceases to change, then U_{mf} would be approximately 4.5 mm/s. As will be seen below, however, significant velocity fluctuations at a point well above the distributor were first observed at $U_s \approx 1.67$ mm/s. This and the visual observations described above suggest that substantial fluidization of the bed occurred nearer the lower of the two possible minimum fluidization velocities, giving $U_{mf} \approx 1.45$ mm/s (i.e. $U_{mb} \approx 5U_{mf}$). The size and density characteristics of the particles place them in Group C (i.e. cohesive) of the Geldart classification. However, the behaviour described above suggests that the particles are only weakly cohesive once fluidized and may be more properly thought of as belonging to Geldart Group A except at low superficial velocities (i.e. in the vicinity of and below the minimum fluidization velocity).

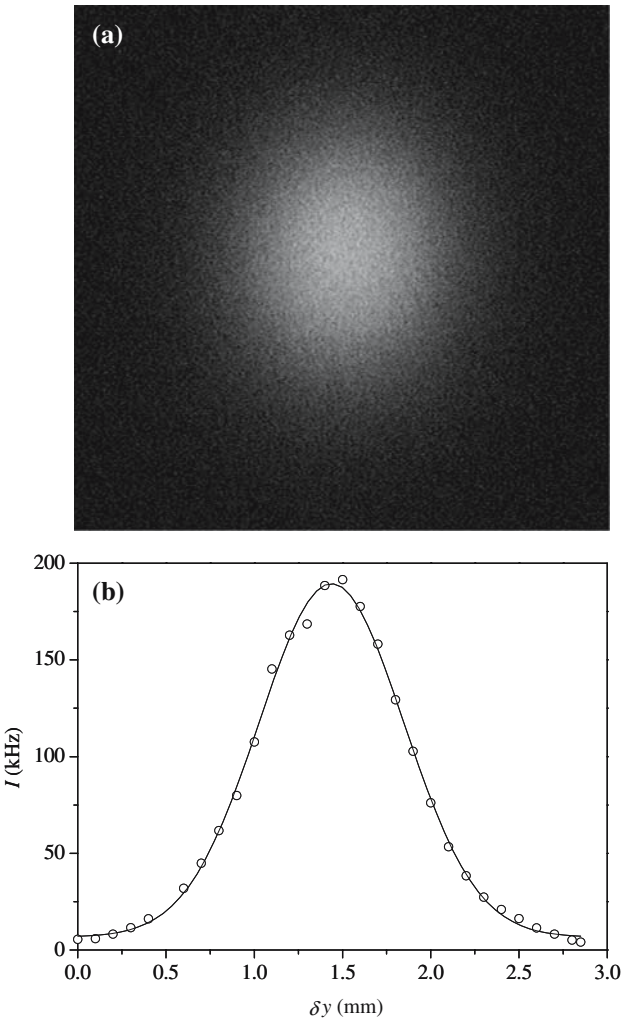

Fig. 5 **a** An example of a diffuse speckle pattern seen on the reverse side of the fluidized bed after the laser light has passed through the bed, and **b** the measured variation of the light intensity from top to bottom of the speckle pattern (*points*) and a Gaussian fit (*line*). The Gaussian fit was integrated to give the total intensity for use in Eq. (6) to determine the transport mean free path, l^*, and mean absorption length, l_a

2.4 Experimental method for determining l^* and l_a

The transport mean free path, l^*, and absorption path length, l_a, were determined at $y = 75$, 150 and 250 mm above the distributor for the relative bed expansions of $(h - h_0)/h_0 = 0.385, 0.538$ and 0.733. As the transmitted light intensity was found to vary little across the bed width, it was assumed that l^* and l_a at a given bed expansion are dependent on height above the distributor only.

The laser was always warmed up for at least 1 h before data collection was begun. As the experiments were done over a number of weeks using a shared facility, all the transmission intensities were measured relative to that of a fully characterised reference latex emulsion. The transmitted light presents as a diffuse speckle pattern on the back of the fluidized beds as seen in Fig. 5a by shifting the optical fibre, this spot was sampled at up to 32 vertical positions 0.1 mm apart, fitted by a Gaussian curve as illustrated in Fig. 5b, and finally integrated to obtain the total transmission for use in Eq. (6).

2.5 Experimental method for determining granular temperature

The intensity autocorrelation function was determined at a number of points in the fluidized bed over a wide range of superficial velocities using both backscattering and transmission modes; granular temperatures obtained from both modes were similar, indicating that the values are in both cases an average through the bed thickness. As indicated above, the sampling points in the bed were targeted by manipulation of the precision stage on which the bed was mounted.

The laser was always warmed up for at least 1 h prior to the onset of intensity data collection. The bed was also run at steady-state for at least 1 h prior to any data being collected. The laser power was modulated for each point prior to

the start of data collection so as to avoid excessive localised heating of the bed whilst maintaining a satisfactory signal-to-noise ratio. Intensity data was collected and correlated in blocks of between 90 and 300 s until the autocorrelation curves remained unchanged (i.e. were repeatable)—this typically required sampling of an hour per point. The electric field autocorrelation and mean square displacement functions were derived off-line from the stored intensity autocorrelation functions using an in-house MATLAB program.

3 Results and discussion

3.1 Transport mean free path and absorption path length

Figure 6, which shows the variation of the transport mean free path with the degree of bed expansion for three heights above the distributor, indicates that the distance a photon must travel before its direction is randomised, l^*, increases in line with the bed voidage increase that accompanies bed expansion. Although l^* was not determined in the packed bed limit (i.e. $(h - h_0)/h_0 \rightarrow 0$) because of unavoidable localised heating problems in the static bed, this figure suggests that the transport mean free path in this case is uniform throughout the bed. The increase in l^* with bed expansion is similar and relatively moderate (less than a doubling) at the two lower positions above the distributor. At $y = 250$ mm, on the other hand, the change in the transport mean free path increases substantially with bed expansion, suggesting the bed expansion is not uniform through the height of the bed – we shall return to this point in more detail later.

The absorption path length was found to vary little and in no systematic way with position or degree of bed expansion. It was, therefore, assumed to be an average of the values determined (i.e. $l_a = 4.11 \pm 0.50$ mm).

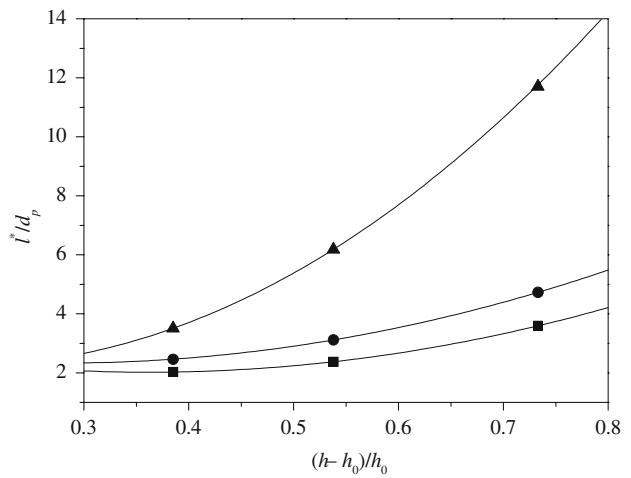

Fig. 6 Variation of transport mean free path (normalised by the particle diameter) with relative bed expansion for $y = 75$ mm (*square*), $y = 150$ mm (*circle*) and $y = 250$ mm (*triangle*) above the distributor

3.2 Autocorrelation functions and particle mean square displacement

The example intensity autocorrelation function (IACF) shown in Fig. 7a first decays over the timescale of 10^{-7} to 10^{-6} s from a plateau of $g_2 \approx 1.47$ to a second plateau of $g_2 \approx 1.006$ where it remains until $t \approx 10^{-2}$ s before finally decaying to unity. A double decay such as seen here could indicate that the particle dynamics are characterised by two timescales or, alternatively, slow fluctuations in the power of the laser [64]. By applying the same experimental set-up to a dilute emulsion (5.4% v/v of 290 nm PMMA particles in dodecane), the latter was ruled out by virtue of the fact that the IACF possessed only a single decay. Whilst other non-physical factors cannot be ruled out entirely, it appears as if the particle dynamics at this point in the bed for $U_s = 5$ mm/s are indeed governed by two timescales (these dynamics may not prevail elsewhere in the bed and for other conditions, as is indicated in Abate and Durian [65]); we shall return to the nature of the processes involved when considering the mean square displacement below.

The two timescales seen in the IACF are reflected in the normalised electric field autocorrelation function (FACF) obtained from the IACF using the Siegert relationship as shown in Fig. 7b. The mean square displacement obtained from inversion of Eq. (4) using the FACF, which is shown in Fig. 7c, is characterised by three distinct regions—the ballistic region, which in this case terminates at $\tau_c \approx 1.78$ μs, a region in which the MSD remains unchanged, and a sub-diffusive region at long times where $\langle \Delta r^2 \rangle \sim t^\alpha$ for $\alpha < 1$. The intermediate region suggests the particles spend much time (in this case O(1000) collisions) trapped within cages defined by surrounding particles, a phenomenon previously observed for fluid molecules within porous solids at low temperatures or near the percolation threshold of the pore system [66,67]. The longer term MSD behaviour indicates that whilst the particles at shorter times are locally trapped, over longer times they do in fact displace within the bed, albeit in a way that is suggestive of activated hopping between interstices—it is these dynamics which are characterised by the second decay observed in the autocorrelation functions. Quantitative analysis of the ballistic region of the MSD yields a velocity fluctuation of $\delta v \approx 10.61$ mm/s, a time between successive collisions of $\tau_c \approx 1.78$ μs, and a mean free path of $\lambda_c \approx 18.9$ nm, these times and distances clearly indicate the level of sensitivity of the DWS method.

3.3 Influence of superficial velocity and voidage on granular temperature

Figure 8a shows the variation of the velocity fluctuations with superficial velocity at a point well above the distributor where no significant channelling was observed. The velocity

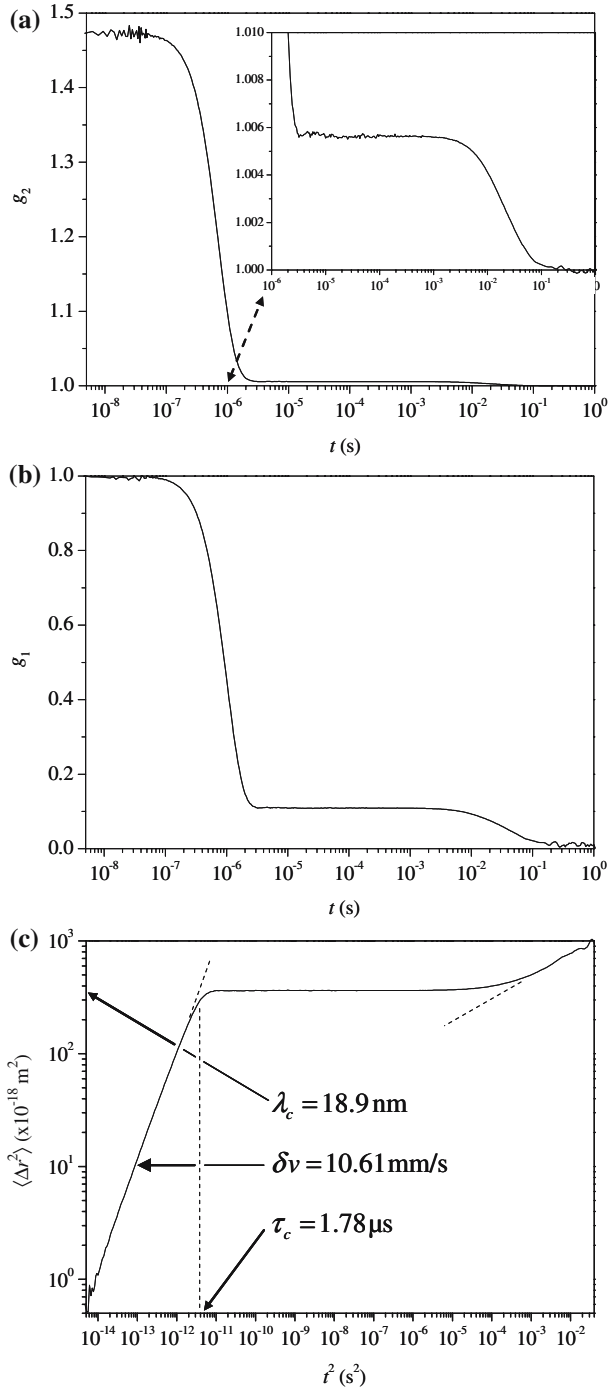

Fig. 7 **a** The intensity autocorrelation function, g_2, evaluated using transmitted intensity data obtained at a point on the centreline of the bed and $y = 150$ mm above the bed distributor for a superficial velocity of $U_s = 5$ mm/s; the insert shows the long-time approach to unity. **b** The normalised electric field autocorrelation function, g_1, obtained from g_2 using the Siegert relationship, Eq. (3). **c** The mean square displacement obtained from g_1 by inverting Eq. (4); the mean free path of the particles, λ_c, the average time between successive collisions, τ_c, and the mean fluctuation velocity, δv, are indicated

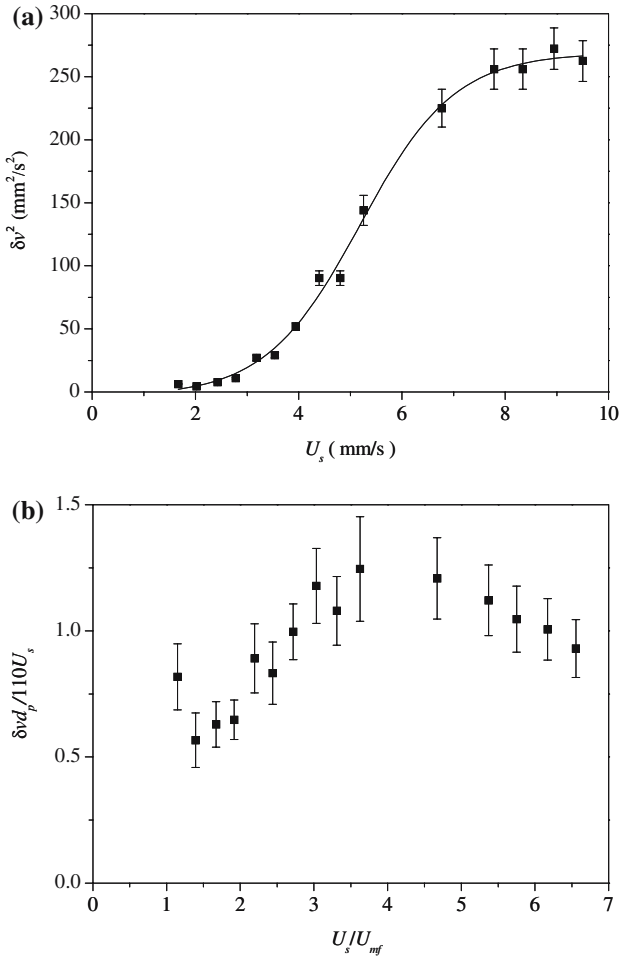

Fig. 8 Square of the velocity fluctuations as a function of superficial velocity at a point 140 mm above the distributor and 45 mm from the edge of the bed. Absence of *error bars* indicates the errors are no greater than the size of the symbol. *Lines* are a guide for the eye only

fluctuations, which were first detected at $U_s \approx 1.67$ mm/s, rise with superficial velocity in a sigmoidal fashion to a plateau in the region of the minimum bubbling velocity, it is clear from this figure that bubbling is *not* necessary for particle fluctuations to exist as asserted by Menon and Durian [48]. The initial rise reflects the increasing energy that is available to the particles from the fluidizing gas as the interstitial gas velocity rises. At the onset of bubbling, however, further increases in gas flow rate pass through the bed as bubbles. The smallness of the number, size and speed of the bubbles in the region of the minimum bubbling velocity means they are expected to have little effect on the particles, which leads to the observed plateau. Although we do not probe well beyond the minimum bubbling velocity (the increasingly large bubbles disrupt data gathering), it is expected that once the number of bubbles and their size and speed increase sufficiently, the velocity fluctuations will once again begin to increase with superficial velocity [34].

Figure 8b shows the velocity fluctuation data presented using the dimensionless group of Cody et al. [46] as discussed in the Introduction to this paper. The plot is very reminiscent

of that obtained by Cody et al. for Geldart Group A particles (see Figs. 7, 8 of their paper), although the initial rise is not as sharp and the maximum is not as great—these differences are perhaps indicative of the cohesive forces that are at play, especially at lower superficial velocities (see Sect. 2.3). The dimensionless data is also O(1), suggesting that the empirical length scale of Cody et al. [46], $d_0 = 110\,\mu\text{m}$, is not obviously inappropriate for the particles being used here.

The variation of the velocity fluctuations with superficial velocity seen in Fig. 8 infact convolutes two effects—the influence of local strain rate and local voidage. We have resorted to the theory of Bachelor [68] for uniform fluidized beds in an effort to separate these two effects. In this theory, it is proposed that the mean particle velocity averaged over a cross-section of a uniform fluidized bed, v, and the fluctuations about this mean, δv, are related by a function of the solid fraction only

$$\delta v^2 = H(\phi)v^2 \tag{7}$$

Noting that in a uniform fluidized bed, $U_s = -(1-\phi)v$ [68], this equation can be re-arranged to obtain

$$\delta v^2 = f(\phi)U_s^2 \tag{8}$$

Unfortunately, as will be seen below, the granular temperature in fact varies across the width of the bed and, therefore, Eq. (8) does not strictly hold here. Accepting this, it is still interesting to see how the function $f(\phi)$ varies at a point in the bed within the limitations of the data available in Figs. 3 and 8. Whilst the function obtained, which is shown in Fig. 9, suffers somewhat from the fluctuations in the original experimental data, it does behave very much as described by Batchelor [68]—it increases sharply from near zero as the solids loading exceeds $\phi \approx 0.33$ to a maximum at $\phi \approx 0.4$ from where it tails off to zero at $\phi \approx 0.53$.

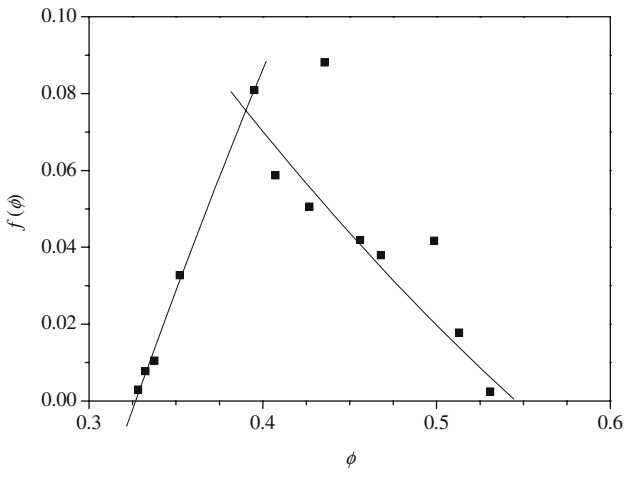

Fig. 9 Function $f(\phi)$ of Eq. (8) as determined by combining the data in Figs. 3 and 8. *Lines* are a guide for the eye only

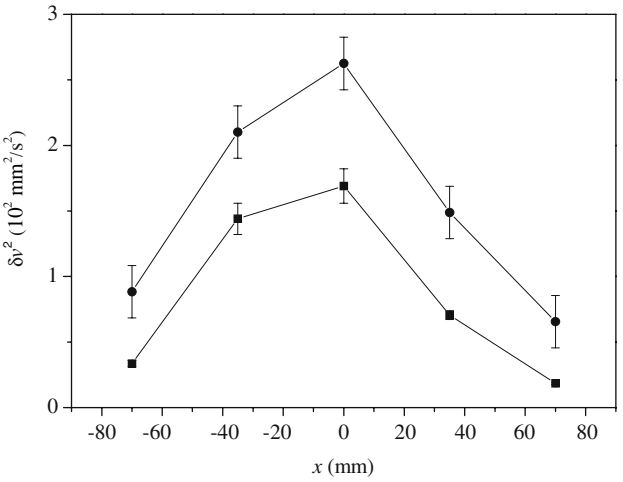

Fig. 10 Square of the velocity fluctuations as a function of position across the bed width ($x = 0$ corresponds to the bed centreline) at $U_s =$ 7.3 mm/s for $y = 75$ mm (*square*) and $y = 150$ mm (*circle*) above the distributor. Absence of *error bars* indicates the errors are no greater than the size of the symbol. *Lines* are a guide for the eye only

3.4 Spatial variation of granular temperature

Figure 10 shows the variation of the velocity fluctuations across the width of the bed, x, at two different heights above the distributor, y, at a superficial velocity where the bed was homogeneously fluidized. This figure indicates that the velocity fluctuations are approximately symmetrical about the centreline where they are also maximal, and that this behaviour does not vary qualitatively with height above the distributor. The variation of the velocity fluctuations across the bed matches the bulk velocity profiles found by Wong [69] using PEPT on a gas FB of similar geometry, suggesting that, at least in directions transverse to the flow, there is a direct relationship between local velocity and velocity fluctuations.

Figure 11 indicates, for a superficial velocity where the bed was homogeneously fluidized, that the velocity fluctuations increase substantially and in a nonlinear manner with height above the distributor. As the bulk velocity does not vary with y, this increase must be due to other factors. One possibility is a variation in voidage with height above the distributor, which is suggested by the data presented in Fig. 6 above. The linear decrease in the pressure with y also shown in Fig. 11 indicates, however, that the solids loading, and hence voidage is uniform, in line with visual observations. The increase of bed transmission with y, which is also shown in Fig. 11, indicates, on the other hand, that the voidage is not uniform *at the scale which is probed by the light*, which corresponds to the transport mean free path, l^*. As backscattering increases with decreasing voidage [59,61], the transmission and pressure results together indicate that the microscopic voidage increases with y whilst the macroscopic voidage remains constant. These two

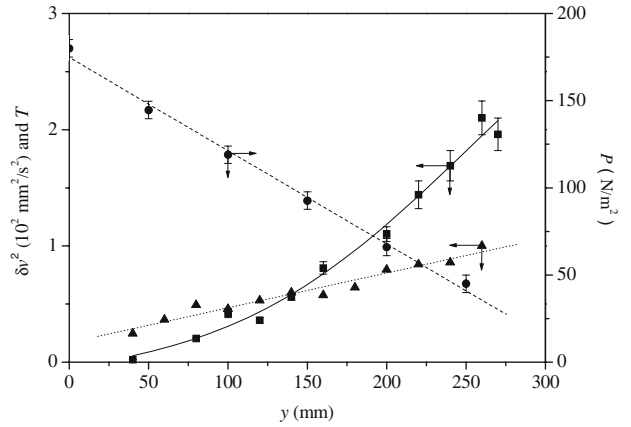

Fig. 11 Square of the velocity fluctuations (*squares*), pressure (*circles*) and transmission of the bed (*triangles*) as a function of height above the distributor at $U_s = 7.3$ mm/s and 45 mm from the edge of the bed. Absence of *error bars* indicates the errors are no greater than the size of the symbol. *Lines* are a guide for the eye only

facts can be reconciled by the existence of clusters of voidage lower than the bed average that decrease in size relative to l^* as y increases. This hypothesis is consistent with the presence of weak cohesive effects at higher superficial velocities as described above, visual observations at low velocities that suggest cohesive effects diminish with height above the distributor, and even other experimental studies, albeit on smaller particles [70–72].

4 Conclusion

Diffusing wave spectroscopy has been used to measure the velocity fluctuations of 60 μm particles in a thin (∼140 particle diameter) non-circulating gas fluidized bed whose superficial velocity and bed expansion at onset of bubbling are significantly greater than at incipient fluidization. The measured velocity fluctuations are an average across the bed thickness (i.e. not confined to the bed wall), and have been determined as a function of the superficial velocity, and at various heights above the distributor and across the bed width. The dynamics of the particles were observed to be characterised by up to two timescales. The first is associated with particles trapped within cages defined by surrounding particles. The second timescale is related to the activated movement of particles between interstices in the bed. Unlike Menon and Durian [48], who also used DWS but with different particles, velocity fluctuations were observed prior to the onset of bubbling. The velocity fluctuations were observed to increase with superficial velocity beyond the minimum fluidization velocity, with the fluctuations being of the same order as the superficial velocity, this variation is both qualitatively and quantitatively in line with that observed by Cody et al. [46] for fine particles. The dimensionless group of Cody and co-workers described in the introduction to this paper was also found to be applicable. Velocity fluctuations were observed to be approximately symmetrically around the centreline where they were maximal, and to increase with height above the distributor; this latter trend is possibly linked to the clustering of the particles at the bottom of the bed.

Acknowledgement We thank the EPSRC (GR/N33485/01 and EP/C546849/1) for support of this research.

References

1. Ogawa, S.: Multitemperature theory of granular materials. In: Cowin, S.C., Satake, M. (eds.) Proceedings of the US-Japan Seminar on Continuum-Mechanical and Statistical Approaches in the Mechanics of Granular Materials, pp. 208–217. Gakujutsu Bunken Fukyukai, Tokyo (1978)
2. Ogawa, S., Umemura, A., Oshima, N.: On the equations of fully fluidized granular materials. J. Appl. Math. Phys. **31**, 483–493 (1980)
3. Jenkins, J.T., Savage, S.B.: Theory for the rapid flow of identical, smooth, nearly elastic, spherical particles. J. Fluid Mech. **130**, 187–202 (1983)
4. Lun, C.K.K., Savage, S.B., Jeffrey, D.J., Chepurniy, N.: Kinetic theories for granular flow: inelastic particles in Couette flow and slightly inelastic particles in a general flowfield. J. Fluid Mech. **140**, 223–256 (1984)
5. Chapman, S., Cowling, T.: The Mathematical Theory of Non-Uniform Gases. Cambridge University Press, Cambridge (1970)
6. Grad, H.: On the kinetic theory of rarefied gases. Comm. Pure Appl. Math. **2**(4), 331–407 (1949)
7. Campbell, C.S.: Rapid granular flows. Ann. Rev. Fluid Mech. **22**, 57–92 (1990)
8. Natarajan, V.V.R., Hunt, M.L.: Kinetic theory analysis of heat transfer in granular flows. Int. J. Heat Mass Trasfer **41**(13), 1929–1944 (1998)
9. Tan, H.S., Goldschmidt, M.J.V., Boerefijn, R., Hounslow, M.J., Salman, A.D., Kuipers, J.A.M.: Population balance modelling of fluidized bed melt granulation. Trans. IChemE **83**(A7), 871–880 (2005)
10. Ding, J., Lyczkowski, R.W.: Three-dimensional kinetic theory modelling of hydrodynamics and erosion in fluidized beds. Powder Technol. **73**(2), 127–138 (1992)
11. Ahn, H., Brennen, C.E., Sabersky, R.H.: Measurements of velocity, velocity fluctuation, density, and stresses in chute flows of granular materials. ASME J. Appl. Mech. **58**(3), 792–803 (1991)
12. Hsiau, S.S., Hunt, M.L.: Shear-induced particle diffusion and longitudinal velocity fluctuations in a granular-flow mixing layer. J. Fluid. Mech. **251**, 299–313 (1993)
13. Boateng, A.A., Barr, P.V.: Granular flow behaviour in the transverse plane of a partially filled rotating cylinder. J. Fluid Mech. **330**, 233–249 (1997)
14. Drake, T.G.: Granular flow: Physical experiments and their implications for microstructural theories. J. Fluid Mech. **225**, 121–152 (1991)
15. Natarajan, V.V.R., Hunt, M.L., Taylor, E.D.: Local measurements of velocity fluctuations and diffusion coefficients for a granular material flow. J. Fluid Mech. **304**, 1–25 (1995)
16. Azanza, E., Chevoir, F., Moucheront, P.: Experimental study of collisional granular flows down an inclined plane. J. Fluid Mech. **400**, 199–227 (1999)
17. Bi, W., Delannay, R., Richard, P., Valance, A.: Experimental study of two-dimensional, monodisperse, frictional–collisional granu-

lar flows down an inclined chute. Phys. Fluids **18**(12), 123302–123314 (2006)
18. Hanes, D.M., Walton, O.R.: Simulations and physical measurements of glass spheres flowing down a bumpy incline. Powder Technol. **109**, 133–144 (2000)
19. Armanini, A., Capart, H., Fraccarollo, L., Larcher, M.: Rheological stratification in experimental free-surface flows of granular-liquid mixtures. J. Fluid Mech. **532**, 269–319 (2005)
20. Hsiau, S.S., Jang, H.W.: Measurements of velocity fluctuations of granular materials in a shear cell. Expt. Thermal Fluid Sci. **17**(3), 202–209 (1998)
21. Hsiau, S.S., Shieh, Y.M.: Effect of solid fraction of fluctuations and self-diffusion of sheared granular flows. Chem. Eng. Sci. **55**(11), 1969–1979 (2000)
22. Hsiau, S.S, Yang, W.L.: Stresses and transport phenomena in sheared granular flows with different wall conditions. Phys. Fluids **14**(2), 612–621
23. Hsiau, S.S., Yang, W.L.: Transport property measurements in sheared granular flows. Chem. Eng. Sci. **60**(1), 187–199 (2005)
24. Yang, W.L., Hsiau, S.S.: Wet granular materials in sheared flows. Chem. Engng. Sci. **60**(15), 4265–4274 (2005)
25. Hsiau, W.L., Lu, L.S., Chen, J.C., Yang, W.L.: Particle mixing in a sheared granular flow. Int. J. Multiph. Flow **31**(7), 793–808 (2005)
26. Perng, A.T.H., Capart, H., Chou, H.T.: Granular configurations, motions, and correlations in slow uniform flows driven by an inclined conveyer belt. Granul. Matter **8**(1), 5–17 (2006)
27. Warr, S., Huntley, J.M., Jacques, G.T.H.: Fluidization of a two-dimensional granular system: experimental study and scaling behavior. Phys. Rev. E **52**(5), 5583–5595 (1995)
28. Wildman, R.D., Huntley, J.M., Hansen, J.-P.: Self-diffusion of grains in a two-dimensional vibrofluidized bed. Phys. Rev. E **60**(6), 7066–7075 (1999)
29. Losert, W., Cooper, D.G.W, Delour, J., Kudrolli, A., Gollub, J.P.: Velocity statistics in excited granular media. Chaos **9**(3), 682–690 (1999)
30. Blair, D.L., Kudrolli, A.: Collision statistics of driven granular materials. Phys. Rev. E **67**(41), 413011–4130112 (2003)
31. Tai, C.H., Hsiau, S.S.: Dynamic behaviours of powders in a vibrated bed. Powder Technol. **139**(3), 221–232 (2004)
32. Baxter, G.W., Olafsen, J.S.: The temperature of a vibrated granular gas. Granul. Material **9**(1–2), 135–139 (2007)
33. Spinewine, B., Capart, H., Larcher, M., Zech, Y.: Three-dimensional Voronoi imaging methods for the measurement of near-wall particulate flows. Exp. Fluids **34**(2), 227–241 (2003)
34. Jung, J., Gidaspow, D., Gamwo, I.K.: Measurement of two kinds of granular temperatures, stresses, and dispersion in bubbling beds. Ind. Eng. Chem. Res. **44**(5), 1329–1341 (2005)
35. Gidaspow, D., Huilin, L.: Collisional viscosity of FCC particles in a CFB. AIChE J. **42**(9), 2503–2510 (1996)
36. Gidaspow, D., Huilin, L.: Equation of state and radial distribution functions of FCC particles in a CFB. AIChE J. **44**(2), 279–291 (1998)
37. Tartan, M., Gidaspow, D.: Measurement of granular temperature and stresses in risers. AIChE J. **50**(8), 1760–1775 (2004)
38. Longo, S., Lamberti, A.: Grain shear flow in a rotating drum. Exp. Fluids **32**(3), 313–325 (2002)
39. Wildman, R.D., Huntley, J.M., Hansen, J.P., Parker, D.J., Allen, D.A.: Single-particle motion in three-dimensional vibrofluidized granular beds. Phys. Rev. E **62**(3), 3826–3835 (2000)
40. Wildman, R.D., Huntley, J.M., Parker, D.J.: Granular temperature profiles in three-dimensional vibrofluidized granular beds. Phys. Rev. E **63**, 061311–061321 (2001)
41. Wildman, R.D., Parker, D.J.: Coexistance of two granular temperatures in binary vibrofluidized beds. Phys. Rev. Lett. **88**(6), 064201–064205 (2002)
42. Wildman, R.D., Huntley, J.M.: Scaling exponents for energy transport and dissipation in binary vibro-fluidized granular beds. Phys. Fluids **15**(10), 3090–3098 (2003)
43. Bhusarapu, S., Al-Dahhan, M.H., Dudukovič, M.P.: Solids flow mapping in a gas–solid riser: mean holdup and velocity fields. Powder Technol. **163**(1–2), 98–123 (2006)
44. Yang, X., Huan, C., Candela, D., Mair, R.W., Walsworth, R.L.: Measurements of grain motion in a dense, three-dimensional granular fluid. Phys. Rev. Lett. **88**(4), 443011–443014 (2002)
45. Huan, C., Yang, X., Candela, D., Mair, R.W., Walsworth, R.L.: NMR experiments on a three-dimensional vibrofluidized granular media. Phys. Rev. E **69**(41), 041302–0413115 (2004)
46. Cody, G.D., Goldfarb, D.J., Storch, G.V., Norris, A.N.: Particle granular temperature in gas fluidized beds. Powder Technol. **87**(3), 211–232 (1996)
47. Menon, N., Durian, D.J.: Diffusing wave spectroscopy of dynamics in a three-dimensional granular flow. Science **275**, 1920–1922 (1997)
48. Menon, N., Durian, D.J.: Particle motions in a gas-fluidized bed of sand. Phys. Rev. Lett. **79**(18), 3407–3410 (1997)
49. Kim, K., Park, J.J., Moon, J.K., Kim, H.K., Pak, H.K.: Solid–liquid transition in a highly dense 3D vibro-fluidized granular system. J. Korean Phys. Soc. **40**(6), 983–986 (2002)
50. Xie, L.: Study of granular temperatures in gas-fluidized beds by diffusing wave spectroscopy (The University of Edinburgh), PhD Thesis (2005)
51. Xie, L., Biggs, M.J., Glass, D., McLeod, A.S., Egelhaaf, S.U., Petekidis, G.: Granular temperature distribution in a gas fluidized bed of hollow microparticles prior to onset of bubbling. Europhys. Lett. **74**(2), 268–274 (2006)
52. Polashenski, W., Chen, J.C.: Normal solid stress in fluidized beds. Powder Technol. **90**(1), 13–23 (1997)
53. Louge, M.Y., Keast, S.C.: On dense granular flows down flat frictional inclines. Phys. Fluids **13**(5), 1213–1233 (2001)
54. Falcon, E., Aumaître, S., Évesque, P., Palencia, F., Lecoutre-Chabot, C., Fauve, S., Beysens, D., Garrabos, Y.: Collision statistics in a dilute granular gas fluidized by vibrations in low gravity. Europhys. Lett. **74**(5), 830–836 (2006)
55. D'Anna, G., Mayor, P., Barrat, A., Loreto, V., Nori, F.: Observing Brownian motion in vibration-fluidized granular matter. Nature **424**, 909–912 (2003)
56. Mayor, P., D'Anna, G., Barrat, A., Loreto, V.: Observing Brownian motion and measuring temperatures in vibration-fluidized granular matter. New J. Phys. **7**, 28 (2005)
57. Mayor, P., D'Anna, G., Gremaud, G., Barrat, A., Loreto, V.: Mechanical spectroscopy of vibrated granular matter. Mat. Sci. Eng. A **442**(1–2), 256–262 (2006)
58. Valverde, J.M., Castellanos, A., Quintanilla, M.A.S.: Self-diffusion in a gas-fluidized bed of fine powder. Phys. Rev. Lett. **86**(14), 3020–3023 (2001)
59. Weitz, D.A., Pine, D.J. : Diffusing wave spectroscopy. In: Brown, W. (ed.) Dynamic Light Scattering, pp. 652–719. OUP, Oxford (1993)
60. Li, J.H., Lisyansky, A.A., Cheung, T.D., Livdan, D., Genack, A.Z.: Transmission and surface intensity profiles in random-media. Europhys. Lett. **22**(9), 675–680 (1993)
61. Leutz, W., Rička, J.: On light propagation through glass bead packings. Opt. Commun. **126**(4–6), 260–268 (1996)
62. Ishimaru, A.: Wave Propagation and Scattering in Random Media. Wiley, IEEE, London (1999)
63. Geldart, D., Wong, A.C.Y.: Fluidization of powders showing degrees of cohesiveness I. Bed Expans. Chem. Eng. Sci. **39**(10), 1481–1488 (1984)
64. Lemieux, P.A., Durian, D.J.: Investigating non-Gaussian scattering processes by using n-th order intensity correlation functions. J. Opt. Soc. Am. A **16**(7), 1651–1664 (1999)

65. Abate, A.R., Durian, D.J.: Approach to jamming in an air-fluidized granular bed. Phys. Rev. E **74**(3), 031308 (2006)
66. Biggs, M., Agarwal, P.: Mass diffusion of atomic fluids in random micropore spaces using equilibrium molecular-dynamics. Phys. Rev. A **46**(6), 3312–3318 (1992)
67. Biggs, M., Agarwal, P.: Mass diffusion of diatomic fluids in random micropore spaces using equilibrium molecular-dynamics. Phys. Rev. E **49**(1), 531–537 (1994)
68. Batchelor, G.K.: A new theory of the instability of a uniform fluidized bed. J. Fluid Mech. **193**, 75–110 (1988)
69. Wong, Y.S.: Experimental and numerical investigation of fluidisation behaviour with and without the presence of immersed tubes. PhD Thesis, pp. 75 (The University of Birmingham) (2003)
70. Morooka, S., Kusakabe, K., Kobata, A., Kato, Y.: Fluidization state of ultrafine powders. J. Chem. Eng. Jpn. **21**(1), 41–46 (1988)
71. Zhao, G.Y., Zhu, C.W., Hlavacek, V.: Fluidization of micron-sized ceramic powders in a small-diameter fluidized bed. Powder Technol. **79**(3), 227–235 (1994)
72. Wang, Z., Kwauk, M., Li, H.: Fluidization of fine particles. Chem. Eng. Sci. **53**(3), 377–395 (1998)